



Modification of the Euler Load for the Stiffened Compressive Members and Determination of the Optimal Stiffening for the Maximum Buckling Load

M. Karimian Sichani^{1*}, A. Keramati² and F. Behzadnia³

1. M.Sc. Graduated of Structural Engineering, Department of Civil and Environmental Engineering, Amirkabir University of Technology, Tehran, Iran.
2. Retired Assistant Professor, Department of Civil and Environmental Engineering, Amirkabir University of Technology, Tehran, Iran.
3. PhD student of Structural Engineering, Department of Civil and Environmental Engineering, Amirkabir University of Technology, Tehran, Iran.

Corresponding author: mahsakarimian@aut.ac.ir

ARTICLE INFO

Article history:

Received: 14 February 2020

Accepted: 29 July 2020

Keywords:

Stiffener length,
Critical load,
Moment of inertia,
Variable cross section,
Buckling.

ABSTRACT

The potential of buckling in compressive members has been considered as a disadvantage when using steel members in the construction industry. In spite of the progress made in this regard, buckling is still considered as a challenge in the analysis and design of compressive steel structural members. Such a challenging phenomenon can be controlled by strengthening of compressive members. Stiffened compressive members can control the weakness of steel members in the global buckling. In this paper, elastic buckling behavior of three-segment symmetric steel members with pinned ends is investigated. The differential stability equation for non-prismatic three-segment members is solved numerically. Critical load parameter for stiffened members is calculated considering different stiffened length and moment of inertia ratios. Based on a wide range of the calculated data, the buckling load could be accounted as a safe measure to be used in the design formulas. Evaluation of the effects of various parameters on the buckling load shows that the desired buckling load value can be achieved by a partially stiffened member. By constant increase of a member's weight, the shorter the length of the variation in the cross-section, the higher moment of inertia is essential in the stiffened segment; and the maximum critical load parameter is achieved by a stiffened length ratio between 0.4 and 0.6.

1. Introduction

The stability analysis of the structural members with variable cross-section is not a

straightforward process due to the difficulty of the complex governing differential equations of such members. Furthermore, the design formulas cited in the building design

codes are determined for the members with constant cross-section. As a result, evaluating non-prismatic compressive steel members for analysis and design purposes is essential. Many engineers prefer to use variable cross-sections or stiffened members in order to decrease the cost and weight of the building. One of the strategies applied for stiffening a compressive steel member is known as welding steel plates to some specific parts over its length, thereby having a member with variable cross-section. Strengthening a member by this strategy leads to a considerable increase in the buckling load of such members. Also this process can be used for rehabilitation purposes.

Numerous studies have been conducted on the assessment of global buckling behavior in non-prismatic steel members. In 1961, Timoshenko and Gere used the column design curves based on the tangent modulus to calculate the approximate non-elastic buckling load of non-uniform bars [1]. Arbabi and Li proposed a semi-analytical procedure for members with variable cross-sections which turned the governing equation of such members into an integral equation; they calculated the critical load of a member with two-segment section, utilizing this approach [2]. The accuracy and flexibility of this procedure for all types of variation in the cross-section and boundary conditions were approved through comparison between the available approaches. Elishakoff and Rollet assessed a column with variable stiffness distribution and came up with close-form solutions for global buckling of the assumed member with the aid of MATHEMATICA computational program [3]. Li presented an exact solution for global buckling of a non-prismatic column with spring supports under both concentrated and distributed loads. This approach was verified by FEM method and

was proved to be accurate and efficient [4]. Al-Sadder derived the exact stability functions for beam-column members with variable cross-sections by which one can determine the tangent stiffness matrix of such sections and therefore conduct an accurate geometric nonlinear analysis (P- Δ) of frames containing members with variable-cross sections [5]. Rahai and Kazemi introduced a procedure for conducting global buckling analysis of tapered columns in which the buckling loads were derived using the modified vibration mode shape and energy methods [6]. Coskun and Atay implemented the variational iteration method (VIM) which is efficient for solving nonlinear differential and integral equations, in order to calculate the critical buckling loads of columns with different types of supports and different variations in cross-sections [7]. Darbandi et al. investigated the static stability of non-uniform columns by implementing a solution based on the singular perturbation method and determination of critical buckling loads and corresponding mode shapes [8]. In 2011, Huang and Li presented a solution for solving the global buckling instability of axially graded Euler-Bernoulli columns with variable cross-sections, considering different boundary conditions. This solution was based on reducing the governing differential equation of buckling to a Fredholm integral equation [9]. Marques et al. proposed a design development for in-plane flexural buckling of linear tapered columns under constant axial forces [10]. Konstantakopoulos et al. numerically solved the governing equation of the global buckling issue considering three types of cross-sections consisting of parabolic, tapered, and stepped sections and applying concentric and eccentric axial forces and concentrated moments at the ends or intermediate points of

the member [11]. Avraam and Fasoulakis evaluated the effects of variation in the cross-sections of columns coupled with the geometric (ratios of length and moment of inertia) and load parameters (the eccentricity) on the pushover analysis results of a frame [12]. Cristutiu et al. conducted an experiment on the tapered members with various web thicknesses, slenderness values, and types of restraints and the results were compared to the results derived from the FEM analysis of such members. It was demonstrated that the analytical solutions provide conservative results in comparison with the actual results derived from the tests [13]. Saljooghi et al. performed the vibration and buckling analysis of functionally graded beams considering various boundary conditions [14]. Hadinafard et al. evaluated the buckling capacity and inelastic behavior of bracing gusset plates with emphasis on the effects of using stiffeners [15]. There are numerous other assessments and studies recently done on the buckling and stability analysis of different types of steel members [16-29].

This study has been performed so that its results could be used for design purposes. Also due to the complexity involved in solving the differential equation, it has been solved numerically to be used by engineers for design of structural members.

In this paper, the methodology applied for calculation of the buckling load of members with variable cross-section is discussed which is similar to that used by Timoshenko. The reason for incorporating this method was its relatively easier solution for a wide range of data with respect to other methods for software.

The stability differential equation for the three-segment non-uniform symmetric

members is numerically solved with the aid of MATHEMATICA computational program and verified by ABAQUS software.

The elastic buckling load of a member is determined considering various stiffened length ratios and different ratios for the increase in the moment of inertia. Such data can be used for design purposes due to the wide range of calculated buckling loads. The calculated data can be safely used for determining the elastic buckling load for design purposes due to the verifications done in this paper.

However, the relationship between the elastic buckling load and the critical load is essential for a designer to determine the critical load. Thus design of a compressive member requires application of accurate experimental tests. In other words, accurate experimental tests are required in order to determine the column curves associated with non-uniform members.

Furthermore, the elastic buckling behavior of the three-segment symmetric compressive members with pinned-ends is evaluated and the corresponding curves and tables are drawn in order to determine the required parameters for modeling, analysis, and design of the stiffened members.

2. Differential Equation

Although the two end displacements of an element with hinged supports are not effective on the stability equations, they are considered and applied in the equations, as shown in Fig.1. It is assumed that δ is equivalent to the relative end displacement of an element perpendicular to its axis and its deformation is relative to the connecting line of the two ends.

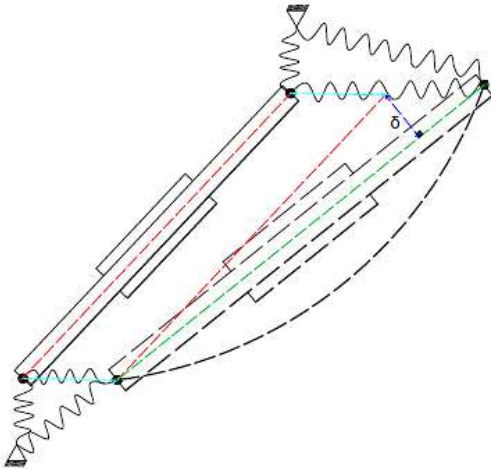


Fig.1. Deformed shape of the member.

Flexural stiffness of the stiffened segment, stiffener length, total length, and flexural stiffness of the unstiffened segment are denoted by EI_{st} , L_{st} , L and EI , respectively.

The equilibrium equation is written for the deformed shape of the member and the boundary conditions are satisfied for each segment. The solution of this equation for the first segment is as [1]:

$$y_1 = a_1 \sin(k_1 x) + a_2 \cos(k_1 x) + \delta x / L \quad (1)$$

$$y_1' = a_1 k_1 \cos(k_1 x) - a_2 k_1 \sin(k_1 x) + \delta / L \quad (2)$$

By applying the initial boundary condition, which is $y_1=0$ at $x=0$, equation (3) can be written as:

$$a_2 = 0 \quad (3)$$

Then the boundary condition at the end of the segment is applied, which is $y_1=y_{1,end}$ at $x=(L-L_{st})/2$. Equations (4) and (5) can be written as follows:

$$y_{1,end} = a_1 \sin\left(k_1 \frac{L-L_{st}}{2}\right) + \delta \frac{L-L_{st}}{2L} \quad (4)$$

$$y_{1,end}' = a_1 k_1 \cos\left(k_1 \frac{L-L_{st}}{2}\right) + \frac{\delta}{L} \quad (5)$$

For the middle segment, the initial boundary condition which is $y=y_{2,0}$ at $x=(L-L_{st})/2$, is applied, then equations (6) and (7) can be written as:

$$y_{2,0} = b_1 \sin\left(k_2 \frac{L-L_{st}}{2}\right) + b_2 \cos\left(k_2 \frac{L-L_{st}}{2}\right) + \delta \frac{L-L_{st}}{2L} \quad (6)$$

$$y_{2,0}' = b_1 k_2 \cos\left(k_2 \frac{L-L_{st}}{2}\right) - b_2 k_2 \sin\left(k_2 \frac{L-L_{st}}{2}\right) + \frac{\delta}{L} \quad (7)$$

The boundary condition at the end of the stiffened segment, which is $y=y_{2,end}$ at $x=(L+L_{st})/2$, is applied, then equations (8) and (9) can be written as:

$$y_{2,end} = b_1 \sin\left(k_2 \frac{L+L_{st}}{2}\right) + b_2 \cos\left(k_2 \frac{L+L_{st}}{2}\right) + \delta \frac{L+L_{st}}{2L} \quad (8)$$

$$y_{2,end}' = b_1 k_2 \cos\left(k_2 \frac{L+L_{st}}{2}\right) - b_2 k_2 \sin\left(k_2 \frac{L+L_{st}}{2}\right) + \frac{\delta}{L} \quad (9)$$

For the third segment, the initial boundary condition (which is $y=y_{3,0}$ at $x=(L+L_{st})/2$), is applied, then equations (10) and (11) are derived:

$$y_{3,0} = c_1 \sin\left(k_1 \frac{L+L_{st}}{2}\right) + c_2 \cos\left(k_1 \frac{L+L_{st}}{2}\right) + \delta \frac{L+L_{st}}{2L} \quad (10)$$

$$y_{3,0}' = c_1 k_1 \cos\left(k_1 \frac{L+L_{st}}{2}\right) - c_2 k_1 \sin\left(k_1 \frac{L+L_{st}}{2}\right) + \frac{\delta}{L} \quad (11)$$

The boundary condition at the end of the member, (or the third segment), is $y=y_{3,end}$ at $x=L$, then equation (12) can be written as:

$$y_{3,end} = c_1 \sin(k_1 L) + c_2 \cos(k_1 L) + \delta \quad (12)$$

By equalizing the boundary conditions ($Y_{1,end} = Y_{2,0}$, $Y_{2,end} = Y_{3,0}$, $Y_{3,end} = \delta$, $Y'_{1,end} = Y'_{2,0}$, $Y'_{2,end} = Y'_{3,0}$), equations (13) to (17) can be written as follows:

$$a_1 \sin\left(k_1 \frac{L-L_{st}}{2}\right) - b_1 \sin\left(k_2 \frac{L-L_{st}}{2}\right) - b_2 \cos\left(k_2 \frac{L-L_{st}}{2}\right) = 0 \quad (13)$$

$$a_1 k_1 \cos\left(k_1 \frac{L-L_{st}}{2}\right) - b_1 k_2 \cos\left(k_2 \frac{L-L_{st}}{2}\right) + b_2 k_2 \sin\left(k_2 \frac{L-L_{st}}{2}\right) = 0 \quad (14)$$

$$b_1 \sin\left(k_2 \frac{L+L_{st}}{2}\right) + b_2 \cos\left(k_2 \frac{L+L_{st}}{2}\right) - c_1 \sin\left(k_1 \frac{L+L_{st}}{2}\right) - c_2 \cos\left(k_1 \frac{L+L_{st}}{2}\right) = 0 \quad (15)$$

$$b_1 k_2 \cos\left(k_2 \frac{L+L_{st}}{2}\right) - b_2 k_2 \sin\left(k_2 \frac{L+L_{st}}{2}\right) - c_1 k_1 \cos\left(k_1 \frac{L+L_{st}}{2}\right) + c_2 k_1 \sin\left(k_1 \frac{L+L_{st}}{2}\right) = 0 \quad (16)$$

$$c_1 \sin(k_1 L) + c_2 \cos(k_1 L) = 0 \quad (17)$$

By setting equal to zero the matrix of coefficient associated with the abovementioned equations, equation (18) is derived using the "MATHEMATICA" computational program:

$$2k_1 k_2 \cos(k_2 L_{st}) \sin(k_1 (L - L_{st})) + (k_1^2 - k_2^2 + (k_1^2 + k_2^2) \cos(k_1 (L - L_{st}))) \sin(k_2 L_{st}) = 0 \quad (18)$$

Where $k_1^2 = P/EI$ and $k_2^2 = P/EI_{st}$ (where P is the axial load); moreover, the parameters such as $n = EI_{st}/EI$, namely the moment of

inertia ratio, $s = L_{st}/L$, which is called the stiffened length ratio, and $\lambda = PL^2/EI$, which is the critical load parameter, are defined. Using these parameters and the "MATHEMATICA" computational program, equation (18) is turned into a dimensionless one:

$$n^{0.5} \cos\left(s \left(\frac{\lambda}{n}\right)^{0.5}\right) \sin(\lambda^{0.5} (1-s)) + (-0.5 + 0.5n + (0.5 + 0.5n) \cos(\lambda^{0.5} (1-s))) \sin\left(s \left(\frac{\lambda}{n}\right)^{0.5}\right) = 0 \quad (19)$$

Equation (19) is numerically solved and the results are shown in Table 1. In this table, the critical load parameter is presented with respect to different values of the moment of inertia and the stiffened length ratios. According to the definition of the critical load parameter, this parameter is directly related to the buckling load and the length of the member and is inversely related to the flexural stiffness.

As is seen in Table 1, with increase in the stiffened length ratio or the moment of inertia ratio, the critical load parameter, and thereby the buckling load would increase.

3. Evaluation of the Effects of "n" and "s" Separately on the Critical Load Parameter

Taking the moment of inertia ratio as constant, the stiffened length variation curves corresponding to the critical load parameter are drawn. This is done to determine increase in the critical load parameter values with respect to the stiffener length ratio. This variation is depicted in Fig. 2.

Table 1. The critical load parameter values for different stiffener length and moment of inertia ratios.

"n" values	"s" values								
	0	0.2	0.3	0.4	0.5	0.6	0.7	0.8	1
1	9.8696	9.8696	9.8696	9.8696	9.8696	9.8696	9.8696	9.8696	9.8696
1.25	9.8696	10.689	11.0955	11.4709	11.7918	12.0393	12.2057	12.2971	12.337
1.5	9.8696	11.3029	12.0765	12.8388	13.5322	14.096	14.4888	14.7082	14.8044
1.75	9.8696	11.7785	12.8757	14.0144	15.1087	16.0436	16.7188	17.1027	17.2718
2	9.8696	12.1571	13.537	15.0315	16.5379	17.8862	18.8955	19.4806	19.7392
2.25	9.8696	12.4654	14.0921	15.9172	17.8353	19.6283	21.0192	21.8416	22.2066
2.5	9.8696	12.7211	14.5639	16.6935	19.0149	21.2745	23.09	24.1855	24.674
2.75	9.8696	12.9364	14.9692	17.378	20.0896	22.8295	25.1082	26.5122	27.1414
3	9.8696	13.1202	15.321	17.9851	21.0707	24.298	27.074	28.8215	29.6088
3.5	9.8696	13.4172	15.9006	19.0121	22.7912	26.9942	30.8505	33.3873	34.5436
4	9.8696	13.6465	16.3576	19.8452	24.2442	29.3996	34.424	37.8815	39.4784
5	9.8696	13.9775	17.0311	21.109	26.5469	33.4709	40.9851	46.6507	49.348
7.5	9.8696	14.4372	17.9925	22.9838	30.1728	40.561	54.321	64.2473	74.022
10	9.8696	14.675	18.5013	24.0063	32.2453	44.9778	64.1223	85.8799	98.696

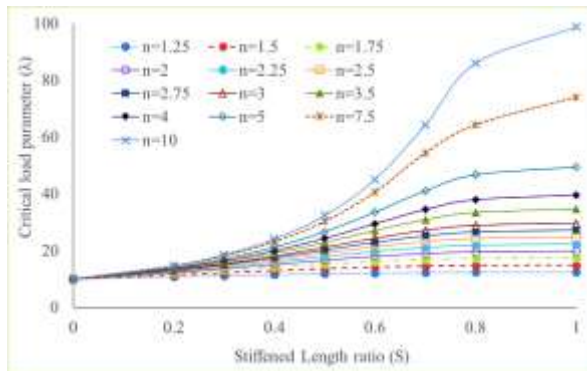


Fig.2. Variation of the critical load parameter with respect to the different stiffened length ratios.

It is evident in Fig.2 that assuming the moment of inertia ratio to be constant, the increase in the stiffened length ratio leads to increase in the critical load parameter and consequently, the buckling load.

In other words, the ratio of the stiffener length to the member’s length is considered to be constant. The curves depicting the critical load parameter corresponding to the ratio of increase in the moment of inertia (n), are drawn in Fig.3 in order to demonstrate the increase in the critical load parameter as a

result of increase in the moment of inertia ratio.

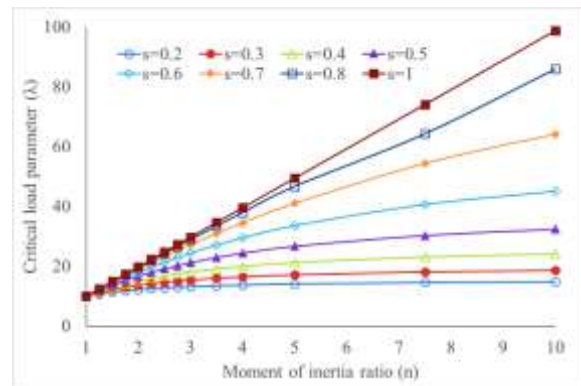


Fig.3. Variation of the critical load parameter with respect to the moment of inertia ratio.

4. Verification of Equation (19) Where no Stiffeners are Used

In order to evaluate equation (19), it is rewritten for the state in which there is no stiffener. In other words, it can be said that $s=0$ and $n=1$.

$$\sin\left(L\left(\frac{P}{EI}\right)^{0.5}\right) = 0 \rightarrow P = \frac{\pi^2 EI}{L^2} \tag{20}$$

It is seen that assuming $n=1$ and $s=0$ in equation (19), equation (27) is derived which represents the axial buckling load in members with no stiffeners as proved previously [1]. Therefore, it is safe to say that equation (19) is accurate for this case.

5. Verification of Equation (19) Where Stiffeners are Used

According to Timoshenko and Gere's research, the critical load is represented by equation 21 [1] where "m" denotes the critical load parameter derived and shown in Table 1.

$$P_{cr} = \frac{mEI}{L^2} \quad (21)$$

Different values for the "m" parameter, (referring to Timoshenko and Gere, for a three-segment member with two end hinges) are given in Table 2 in which I_2/I_1 ratio corresponds to the "n" values.

Table 2. Critical load parameter values according to Timoshenko and Gere's research [1].

I_2/I_1	"s" values			
	0.2	0.4	0.6	0.8
0.01	15.344	27.052	59.843	225.706
0.1	14.675	24.006	44.978	85.88
0.2	13.978	21.109	33.471	46.651
0.4	12.721	16.694	12.275	24.186
0.6	11.632	13.642	15.406	16.306
0.8	10.689	11.471	12.039	12.297

Comparing and matching Table 2 with the definitions and discussions represented in this paper, Table 3 could be derived which demonstrates the critical load parameter values with respect to the aforementioned "n" and "s" values.

Table 3. Critical load parameter "λ" with respect to "s" and "n" values.

"n" values	"s" values			
	0.2	0.4	0.6	0.8
100	15.344	27.052	59.843	225.706
10	14.675	24.006	44.978	85.88
5	13.978	21.109	33.471	46.651
2.5	12.721	16.694	12.275	24.186
1.67	11.632	13.642	15.406	16.306
1.25	10.689	11.471	12.039	12.297

Comparing the critical load parameters obtained and shown in Table 1 with the values represented in Table 3, it can be seen that the critical load parameters derived by numerical solution of equation (19), introduced in this paper, are equal to the factor m, represented in Timoshenko's research. Therefore, it can be said application of equation (19) leads to accurate results.

6. Verification of equation (19) using ABAQUS software

For verification of the calculated buckling load for global buckling, a structural member with 500 cm length and assuming $S=0.5$ and $n=1.5$ has been modeled. The buckling load using the solved equation and the proposed method is 55925 kg, and the buckling load using the FEM method in ABAQUS software is 55404 kg. Comparing the results, one could see the good accuracy of the solved equation. Fig.4 shows the model used in the software.

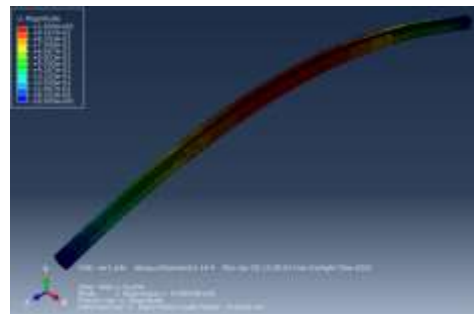


Fig.4. Model of a member in ABAQUS software.

7. Evaluation of the Effects of Cross-Section Parameters on the Buckling Capacity

In this section, the effects of changing the length, width, and thickness of the section on the buckling capacity of the member is assessed through considering change in the weight of the cross-section as the parameter

which is effective on the economic evaluation.

If the equivalent critical load for the member with variable cross-section is written with respect to the equivalent moment of inertia, equation (20) can be written as follows:

$$P_{cr} = \frac{\pi^2}{L^2} EI_{eq} \tag{22}$$

Table 4. The ratio of equivalent to the initial moment of inertia corresponding to various stiffened length ratios and moments of inertia ratios.

"n" values	"s" values								
	0	0.2	0.3	0.4	0.5	0.6	0.7	0.8	1
1	1	1	1	1	1	1	1	1	1
1.25	1	1.083023	1.12421	1.162246	1.19476	1.219837	1.236697	1.245957	1.25
1.5	1	1.145224	1.223606	1.300843	1.371099	1.428224	1.468023	1.490253	1.5
1.75	1	1.193412	1.304582	1.419956	1.530832	1.625557	1.693969	1.732867	1.75
2	1	1.231772	1.371585	1.52301	1.67564	1.812252	1.914515	1.973798	2
2.25	1	1.26301	1.427829	1.61275	1.807095	1.988763	2.129691	2.213018	2.25
2.5	1	1.288917	1.475632	1.691406	1.926613	2.155558	2.339507	2.450505	2.5
2.75	1	1.310732	1.516698	1.76076	2.035503	2.313113	2.543994	2.686249	2.75
3	1	1.329355	1.552343	1.822272	2.134909	2.461903	2.743171	2.92023	3
3.5	1	1.359447	1.611068	1.926329	2.309232	2.735086	3.125811	3.382842	3.5
4	1	1.38268	1.657372	2.01074	2.456452	2.978804	3.487882	3.8382	4
5	1	1.416217	1.725612	2.13879	2.689765	3.391313	4.152661	4.726706	5
7.5	1	1.462795	1.823022	2.328747	3.057145	4.10969	5.50387	6.509615	7.5
10	1	1.486889	1.874574	2.432348	3.267133	4.557206	6.49695	8.701457	10

In equation (20), P_{cr} is equal to the buckling load of the stiffened member, and EI_{eq} is the equivalent moment of inertia of the member with variable cross-section.

$$\lambda = \frac{P_{cr} L^2}{EI} \tag{23}$$

Combining equations (22) and (23) results in equation (24) which is written as follows:

$$\lambda = \frac{\pi^2 EI_{eq}}{EI} \tag{24}$$

Equation (24) shows that the critical load parameter for the members with a constant cross-section, where $EI_{eq}=EI$, is equal to π^2 .

Table 4 demonstrates the ratio of $EI_{eq}/EI = \lambda / \pi^2$ which can be used to determine the

critical load required for the design of a compressive member.

In order to determine the equivalent section area of the member, the compatibility equations of axial deformation, available in the references [30], are used.

If the initial section area, the total section area in the stiffened area, and the stiffener length ratio are denoted by A , A_{st} , and s , respectively, the axial deformation of a member with constant section area, represented by A_{eq} , and the total length represented by L , can be determined by equation (25):

$$\frac{L}{EA_{eq}} = \frac{L - L_{st}}{EA} + \frac{L_{st}}{EA_{st}} \quad (25)$$

Therefore, the equivalent section area is determined by equation (26):

$$A_{eq} = \frac{AA_{st}}{A_{st}(1-s) + As} \quad (26)$$

The equivalent radius of gyration is given by equation (27):

$$r_{eq} = \sqrt{\frac{I_{eq}}{A_{eq}}} \quad (27)$$

The equivalent slenderness ratio for buckling of the member with the variable cross-section is expressed by equation (28):

$$\lambda_{eq} = \frac{KL}{r_{eq}} \quad (28)$$

The overweight resulting from adding plates is equal to:

$$\Delta W = 2sL \times A_p \times \rho \quad (29)$$

In this equation A_p is the cross section of each stiffener and ρ is density of the material of the cross-section, which is equal to 7850 kg/m³ for steel. Assuming different values for Δw , A_p can be calculated using equation (29) for different stiffener lengths. In addition, denoting the width of the stiffener by "d", the thickness of the stiffener, "t", can be calculated. Consequently, with the aid of equation (30), the stiffened cross-sectional moment of inertia is calculated. In this equation, "e" represents equivalent to the free distance between two parts of the section and "b" is equal to the width of the section.

$$\Delta I_{yy} = 2 \left(\frac{dt^3}{12} + dt \times \left(\frac{b+e+t}{2} \right)^2 \right) \quad (30)$$

Assuming a percentage increase in the ratio of the moment of inertia of the stiffened segment to the moment of inertia of the basic section, λ can be calculated using Table 1. Then, λ / π^2 can be calculated using Table 4 for different values of "s" and "n".

As an example Table 5, is drawn for a double channel 8, assuming a constant increase in weight, and all the above-mentioned steps are applied for this section.

In Fig.5, variation of the length of the stiffener with respect to the increased moment of inertia in stiffened segment is plotted, considering a constant increase in weight. According to this figure, it can be seen that with a constant increase in the weight of the section, the smaller the length of modification in the cross-section, the higher moment of inertia is required for the stiffened segment.

Table 5. Sample calculations for different lengths of stiffener for a constant increase in weight equal to 5%.

ΔW (%)	Section	h (cm)	A (cm ²)	I_{yy} (cm ⁴)	s	A_p (cm ²)	d (cm)	t (cm)	ΔI_{yy} (cm ⁴)	$\Delta I_{yy}\%$	I_{yy} new (cm ⁴)	n	λ	EI_{eq}/EI	$\Delta\lambda$ %
0.05	2U8	8	22	212	0.2	2.75	8	0.34	88.6	41.8	300.6	1.42	11.12	1.13	12.66
0.05	2U8	8	22	212	0.3	1.83	8	0.23	58.8	27.7	270.8	1.28	11.21	1.14	13.62
0.05	2U8	8	22	212	0.4	1.38	8	0.17	44.1	20.8	256.1	1.21	11.22	1.14	13.67
0.05	2U8	8	22	212	0.5	1.10	8	0.14	35.2	16.6	247.2	1.17	11.17	1.13	13.16
0.05	2U8	8	22	212	0.6	0.92	8	0.11	29.4	13.8	241.4	1.14	11.09	1.12	12.32
0.05	2U8	8	22	212	0.7	0.79	8	0.10	25.2	11.9	237.2	1.12	10.98	1.11	11.30
0.05	2U8	8	22	212	0.8	0.69	8	0.09	22.0	10.4	234.0	1.10	10.88	1.10	10.23

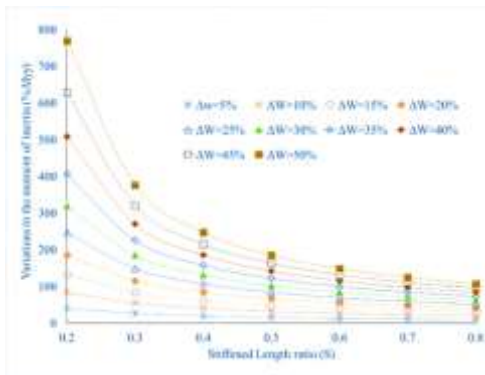


Fig.5. Change in the length of the stiffener corresponding to increased moment of inertia, considering a constant increase in weight.

In Fig.6, the change in the length of the stiffener with respect to the critical load parameter is plotted, considering a constant increase in weight (ΔW). According to this figure, it is evident that with a constant increase of weight, the maximum value of increase (in percentage) in the critical load parameter for a member is derived when the stiffened length ratio has a value between 0.4 and 0.6. In other words, for " ΔW "s equal to 5 and 10, the aforementioned value (peak value of $\Delta\lambda$) is derived equal to 0.4 of the length of the member. For " ΔW "s equal to 15, 20, and 25 the same quantity is reached at half of the member's length; and for " ΔW "s equal to 30, 35, 40, 45, and 50, the peak value of $\Delta\lambda$ is derived at 0.6 of the total length of the member.

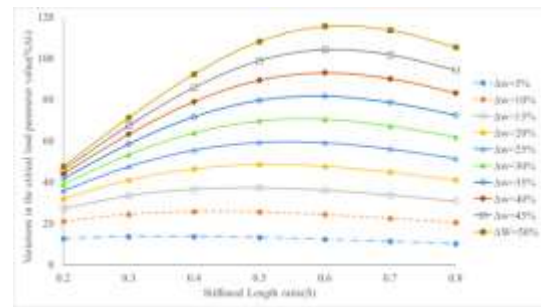


Fig.6. Change in the length of the stiffener with respect to the critical load parameter considering a constant increase in weight.

As an example, by assuming a constant increase in the critical load parameter value, different stiffened length ratios are derived which are shown in Table 6.

Fig.7 shows variation of the length of the stiffener with respect to the moment of inertia for the constant critical load parameter.

Table 6. Stiffened length ratios with respect to the critical load parameter with a constant increase of 10%

s	n	ΔI_{yy}	λ
0.2	1.31	31.18	1.10
0.3	1.20	19.66	1.10
0.4	1.15	14.93	1.10
0.5	1.13	12.53	1.10
0.6	1.11	11.21	1.10
0.7	1.10	10.49	1.10
0.8	1.10	10.14	1.10

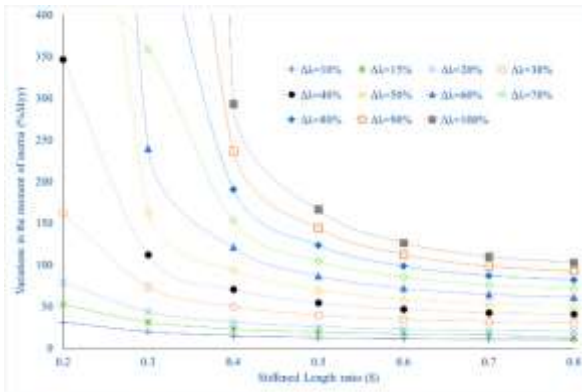


Fig.7. Change in the length of stiffener with respect to the moment of inertia for a constant increase in the critical load parameter.

As is shown in Fig.7, considering a constant value for the critical load parameter (λ), the smaller the value of the stiffened length ratio, (i.e. the length of the member which is strengthened by welding plates), the higher moment of inertia is required to achieve the desired value of the critical load parameter. Moreover, it is observed that by increasing the constant value of λ , considering a constant value for the stiffened length ratio (s), the required value of the moment of inertia increases. This point could be observed in Fig.2 as well.

Considering the desired moment of inertia and the length of stiffener, Euler's force is obtained for the member and as a result, the Euler's stress is derived. According to the range of slenderness ratio, the critical stress and finally the capacity of the member could be calculated, referring to the design codes such as AISC360 provided that the relationships governing F_e and F_{cr} are assumed to be the same as given in AISC 360 code. In other words, according to the calculated relations:

$$F_e = \frac{\lambda EI}{AL^2} = \frac{\lambda E}{\left(\frac{L}{r}\right)^2} \quad (31)$$

For unstiffened sections λ is equal to π^2 . According to the calculated table 1, it is found that this value (λ) is greater for all non-prismatic sections than uniform members (π^2) and it is expected that F_{cr} related to this type of sections is greater than this value for the prismatic sections. However, F_{cr} should be obtained by experimental tests.

As a result, tests should be conducted to achieve the curves required for compressive design of non-prismatic members. These design curves depend on the amount and type of imperfection, distribution and amount of residual stresses, support conditions and length of stiffener [7].

8. A design Example for a Particular Compressive Member

It is decided to implement a member with variable cross-section with the base section of 2U26 instead of a constant section comprised of 2U28, such that the alternative section has the same compressive capacity as the initial one. Table 7 represents the geometric properties of a section comprised of 2U28.

For a member with two hinges at two ends K is equal to 1. Therefore, the following equations can be written:

$$\frac{KL}{r_{min}} = \frac{1 \times 408.66}{8.04} = 50.8 \text{ and } 4.71 \sqrt{E/F_y} = 139.3$$

$$F_e = \frac{\pi^2 E}{(KL/r)^2} = \frac{\pi^2 \times 2.1 \times 10^6}{(50.8)^2} = 8030.4 \text{ kg / cm}^2$$

$$\text{and } P_e = F_e \times A_g = 855998 \text{ kg}$$

$$F_{cr} = F_y \times 0.658 \frac{F_y}{F_e} = 2117.8 \text{ kg / cm}^2$$

and $P_{cr} = F_{cr} \times A_g = 225756.3 \text{ kg}$

$W_{total} = 341.6 \text{ kg}$

The weight of the section is equal to:

The geometric properties of the alternative section are represented in Table 8.

Table 7. Geometric properties of a section with 2U28.

Name	Area (cm ²)	I ₃₃ (2I) (cm ⁴)	I ₂₂ (cm ⁴)	r ₃₃ (cm)	r ₂₂ (cm)	L (cm)	w/L (kg/m)
2U28	106.6	12560	6910.2	10.86	8.04	408.66	83.6

Table 8. Geometric properties of the alternative section.

Name	Area (cm ²)	I ₃₃ (2I) (cm ⁴)	I ₂₂ (cm ⁴)	r ₃₃ (cm)	r ₂₂ (cm)	L (cm)	w/L (kg/m)
2U26	96.6	9640	5697	9.99	7.68	408.66	75.8

Half of the member length is considered to be stiffened by two stiffener plates, with 10 cm width and of 1 cm thickness. Table 9 shows the geometric properties of each stiffener.

Table 9. Geometric properties of stiffeners.

d _p (cm)	t _p (cm)	A _p (cm)	s (cm)
10	1	10	0.5

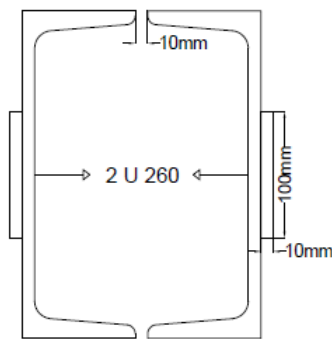


Fig.8. The cross-section of the stiffened alternative member.

For the new stiffened section, the moments of inertia are calculated as follows:

$$I_{33,new} = 9640 + 2 \times (1/12 \times 1 \times 10^3) = 9806.7 \text{ cm}^4$$

$$I_{22,new} = 5703.32 + 2 \times (1/12 \times 1^3 \times 10) + 2 \times (1 \times 10) \times (9 + 1/2 + 0.6)^2 = 7744.9 \text{ cm}^4$$

$$n_{33,new} = I_{33,new} / I_{33} = 1.017 \text{ and}$$

$$n_{22,new} = I_{22,new} / I_{22} = 1.359$$

According to Table 2, considering s=0.5, the ratios of $I_{eq,33}/I_{33}$ and $I_{eq,22}/I_{22}$ which correspond to $n_{33,new}$ and $n_{22,new}$, respectively, are derived. Then, multiplying the derived values by the moment of inertia associated with the section with no stiffener, the moment of inertia of the equivalent section is obtained.

$$I_{eq,33} / I_{33} = 1.013, I_{eq,22} / I_{22} = 1.27324,$$

$$I_{eq,33} = 9933.5 \text{ cm}^4 \text{ and } I_{eq,22} = 7261.7 \text{ cm}^4$$

Based on equation (26), the equivalent section area for the stiffened member is calculated as follows:

$$A_{st} = 2 \times 10 + 96.8 = 116.8 \text{ cm}^2$$

$$A_{eq} = 116.8 \times 96.8 / (116.8 \times (1 - 0.5) + 96.8 \times 0.5) = 105.86 \text{ cm}^2$$

The radius of gyration of the equivalent section is equal to:

$$r_{eq,33} = \sqrt{I_{eq,33}/A_{eq}} = 9.57 \text{ cm and}$$

$$r_{eq,22} = \sqrt{I_{eq,22}/A_{eq}} = 8.18 \text{ cm}$$

$$\frac{KL}{r_{eq,min}} = \frac{1 \times 408.66}{8.18} = 50$$

$$4.71\sqrt{E/F_y} = 139.32$$

$$F_e = \frac{\pi^2 E}{(KL/r_{eq})^2} = \frac{\pi^2 \times 2.1 \times 10^6}{(50)^2} = 8290.5 \text{ kg/cm}^2$$

As it is allowed in the commentary of AISC 360 codes, concerning equations corresponding to a member with constant cross-section and for a non-uniform member, in order to determine the critical load of the member, the relationship between F_{cr} and F_e could be demonstrated as follows where F_{cr} is equal to [31]:

$$F_{cr} = F_y \times 0.658 \frac{F_y}{F_e} = 2126.1 \text{ kg/cm}^2 \Rightarrow$$

$$P_c = F_{cr} \times A_{eq} = 225072 \text{ kg}$$

The weight of this section is equal to:

$$W_{total} = 341.84 \text{ kg}$$

As it is evident in the aforementioned calculations, the derived weights for both the constant and variable cross-section members there is no perceptible difference in spite of approximately having identical compressive capacity values.

If the Euler load of the member with variable cross-section is calculated with reference to Table 1, the Euler loads corresponding to two axes of the section (which are named 2-2 and 3-3) are derived as follows:

$$P_{33} = \frac{EI\lambda}{L^2} = \frac{2.1 \times 10^6 \times 9640 \times 10.00}{408.66^2} = 1212193.8 \text{ kg and}$$

$$P_{22} = \frac{EI\lambda}{L^2} = \frac{2.1 \times 10^6 \times 5703.3 \times 12.55}{408.66^2} = 900046.6 \text{ kg}$$

$$P_{e,min} = 900046 \text{ kg}$$

As a result, the Euler load for the member with variable cross-section is equal to approximately 900 tons which is greater than the same value for a member with constant cross-section (roughly 856 tons). Nevertheless, the critical load (F_{cr}) should be determined through experimental tests. In this example, it is assumed that the relationship between the critical load and the Euler load of a non-uniform member is similar to that of a uniform one. In other words, considering the calculated tables (Table 1 and Table 2), the Euler load is determined as follows:

$$P_e = \frac{EI\lambda}{L^2} \rightarrow F_e = \frac{EI\lambda}{AL^2} \rightarrow F_e = \frac{EI\lambda}{AL^2} = \frac{\lambda E}{(L/r)^2}$$

In the above equation, for uniform members, the value of λ is equal to π^2 . Referring to Table 1, it is evident that the critical load parameter (λ) for the members with variable cross-section is higher than members with constant cross-section. It is expected that the compressive capacity of non-uniform members has a higher value than the uniform ones; nonetheless, the exact value of the critical load (F_{cr}) must be determined by experimental tests.

9. Effect of Imperfection on Compressive Capacity of Members

In this part, using ABAQUS software the effect of imperfection has been studied. Though these relations are prepared for straight and perfect members, but implementing the FEM method, the buckling load for imperfect members with global

buckling mode has been investigated for 12 models. So members, with and without imperfection, have been modeled and the imperfection was equal to maximum allowable imperfection. The buckling load using the FEM method in ABAQUS software has been compared and the error percentage for modeling imperfection has been calculated.

The difference and percentage of error between the analytical solution and buckling load of members with imperfection using FEM method was up to 1.5%.

10. Conclusion

In this paper, the elastic buckling behavior of three-segment symmetric members is investigated. The governing differential stability equation is solved numerically using the MATHEMATICA computational program and the critical load parameter is determined assuming different values for moment of inertia and the stiffened length ratio of the member.

The differential equation is verified considering both states of using no stiffener and where the section is strengthened by stiffeners, referring to the previous research and FEM method. The effects of the change in each parameter including the moment of inertia and the stiffened length ratio on the critical load parameter are assessed, separately. Moreover, considering a constant increase in the weight of the whole member, changes in the moment of inertia and the critical load parameter are depicted by drawing separate curves.

As a result, in a table, the critical load parameter (λ) is presented with respect to different values of the moment of inertia and the stiffened length ratios.

Also in a table, the ratio $EI_{eq}/EI = \lambda / \pi^2$ is demonstrated which can be used to determine the critical load required for design of a compressive member.

According to this research, strengthening some parts of a compressive member is sufficient to achieve the desired value for the critical load parameter. Thereby it is accurate to use the critical load for design purposes, rather than using a uniform section with higher dimensions.

As it is evident, with increase in the stiffened length ratio or the moment of inertia ratio, the critical load parameter and the buckling load would increase. As a result, by increasing the constant value of λ , assuming a constant value for the stiffened length ratio (s), the moment of inertia value increases. Moreover, taking the moment of inertia ratio as constant, the increase in the stiffened length ratio leads to increase in the critical load parameter and consequently, the buckling load.

Furthermore, considering a constant value for increase in the weight of the whole member, the maximum value of the critical load parameter is observed, where the stiffened length ratio is between 0.4 and 0.6. Moreover, it is shown that assuming a constant value for the critical load parameter, the higher the stiffened length ratio, the less moment of inertia is required.

In order to examine the calculated data for design purposes, a design example is given in this paper, in which members with uniform section and variable cross-section are compared to each other. In this example, the column design curves associated with uniform members are applied for the considered non-uniform member as the AISC code allows to be used by designers.

Therefore, the weights of both uniform and non-uniform members showed no noticeable difference despite having roughly the same compressive capacity. In this example, it is shown that the Euler load for a non-uniform member has a greater value than that of a uniform member based on the calculated tables of this study. However, the accurate value of the compressive capacity has to be determined by experimental tests; therefore, the exact relationship between the Euler and critical loads of a non-uniform section could be determined.

Although the global buckling load of members is investigated here, engineers should pay attention to local buckling of members, especially for attaining higher loads.

Symbols

$a_1, a_2, b_1, b_2, c_1, c_2, k_1, k_2$ Constant

parameters

A	Initial section area
A_{eq}	Equivalent section area
A_g	Gross section area
A_p	Cross-section of the stiffener
A_{st}	Total section area in the stiffened area
b	Width of the section
d	Width of the stiffener
d_p	Stiffener depth
e	Free distance between two parts of the section
EI	Flexural stiffness
EI_{st}	Flexural stiffness of the stiffened segment
F_{cr}	Critical stress

F_e	Euler stress
F_y	Yield stress
I	Area moment of inertia
I_{eq}	Equivalent area moment of inertia
K	Effective length factor
L	Total length of the unstiffened segment
L_{st}	Stiffener length
m	Parameter corresponds to the critical load
n	Moment of inertia ratio
P	Axial load
P_{cr}	Critical load
P_e	Euler load
r	radius of gyration
s	Stiffened length ratio
t	Thickness of the stiffener
W	Weight
y	Relative displacement

Greek symbols

Δ	Displacement
δ	Relative end displacement
λ	Slenderness ratio
λ_{eq}	Equivalent slenderness ratio
ρ	Density of the material of the cross-section

REFERENCES

- [1] Timoshenko SP, Gere JM (1961) Theory of elastic stability. New York: McGraw-Hill, 1961.

- [2] Arbabi F, Li F (1991) Buckling of variable cross-section columns: integral-equation approach. *Journal of Structural Engineering* 117 (8):2426-2441
- [3] MATHEMATICA Computational Program.
- [4] Li QS (2000) Buckling of elastically restrained non-uniform columns. *Engineering structures* 22 (10):1231-1243
- [5] Al-Sadder SZ (2004) Exact expressions for stability functions of a general non-prismatic beam-column member. *Journal of Constructional Steel Research* 60 (11):1561-1584
- [6] Rahai AR, Kazemi S (2008) Buckling analysis of non-prismatic columns based on modified vibration modes. *Communications in Nonlinear Science and Numerical Simulation* 13 (8):1721-1735
- [7] Coşkun SB, Atay MT (2009) Determination of critical buckling load for elastic columns of constant and variable cross-sections using variational iteration method. *Computers & Mathematics with Applications* 58 (11-12):2260-2266
- [8] Darbandi SM, Firouz-Abadi RD, Haddadpour H (2010) Buckling of variable section columns under axial loading. *Journal of Engineering Mechanics* 136 (4):472-476
- [9] Huang Y, Li XF (2012) An analytic approach for exactly determining critical loads of buckling of nonuniform columns. *International Journal of Structural Stability and Dynamics* 12 (04):1250027
- [10] Marques L, Taras A, da Silva LS, Greiner R, Rebelo C (2012) Development of a consistent buckling design procedure for tapered columns. *Journal of Constructional Steel Research* 72:61-74
- [11] Konstantakopoulos TG, Raftoyiannis IG, Michaltsos GT (2012) Stability of steel columns with non-uniform cross-sections. *Open Construction and Building Technology Journal* 6:1-7
- [12] Avraam TP, Fasoulakis ZC (2013) Nonlinear postbuckling analysis of frames with varying cross-section columns. *Engineering Structures* 56:1-7
- [13] Cristutiu IM, Nunes DL, Dogariu AI (2013) Steel Members with Variable I Cross Sections under Bending and Compression with Lateral Restraints—Behavior by Experimental Test. In: *Design, Fabrication and Economy of Metal Structures*. Springer, pp 193-198
- [14] Saljooghi R, Ahmadian MT, Farrahi GH (2014) Vibration and buckling analysis of functionally graded beams using reproducing kernel particle method. *Scientia Iranica Transaction B, Mechanical Engineering* 21 (6):1896-1906
- [15] Hadianfard MA, Khakzad AR, Vaghefi M (2015) Analysis of the effect of stiffener on the buckling capacity and non-elastic behavior of bracing gusset plates. *Scientia Iranica Transaction A, Civil Engineering* 22 (4):1449
- [16] Andreev VI, Tsybin NY (2015) On the stability of rod with variable cross-section. *Procedia Engineering* 111:42-48
- [17] Chen Y, Shu G, Zheng B, Lu R (2019) Local buckling behavior of welded π -shaped compression stub columns. *Journal of Constructional Steel Research* 154:224-234
- [18] Couto C, Real PV (2019) Numerical investigation on the influence of imperfections in the local buckling of thin-walled I-shaped sections. *Thin-Walled Structures* 135:89-108
- [19] Dhurvey P (2017) Buckling analysis of composite laminated skew plate of variable thickness. *Materials Today: Proceedings* 4 (9):9732-9736
- [20] He B, Liu D, Long J, Ma L, Ma P (2019) A high order finite strip transfer matrix method for buckling analysis of single-branched cross-section thin-walled members. *Thin-Walled Structures* 135:1-11
- [21] Jiao P, Borchani W, Hasni H, Alavi AH, Lajnef N (2016) Post-buckling response of non-uniform cross-section bilaterally constrained beams. *Mechanics Research Communications* 78:42-50
- [22] Jobbágy D, Ádány S (2017) Local buckling behaviour of thin-walled members with curved cross-section parts. *Thin-Walled Structures* 115:264-276

- [23] Khaniki HB, Hosseini-Hashemi S, Nezamabadi A (2018) Buckling analysis of nonuniform nonlocal strain gradient beams using generalized differential quadrature method. *Alexandria engineering journal* 57 (3):1361-1368
- [24] Kováč M, Baláž I (2019) Stability of centrally loaded members with monosymmetric cross-section at various boundary conditions. *Journal of Constructional Steel Research* 153:139-152
- [25] Yang L, Shi G, Zhao M, Zhou W (2017) Research on interactive buckling behavior of welded steel box-section columns. *Thin-Walled Structures* 115:34-47
- [26] Rezaiee-Pajand M, Shahabian F and Bambaeechee M (2016) Stability of non-prismatic frames with flexible connections and elastic supports. *KSCE Journal of Civil Engineering* 20(2):832-846.
- [27] Rezaiee-Pajand M, Masoodi A, and Bambaeechee M (2018) Tapered beam-column analysis by analytical solution. *Proceedings of the ICE-Structures and Buildings*
- [28] Toosi S, Esfandiari A, and Ranji AR (2019) Buckling Analysis of Tapered Continuous Columns by Using Modified Buckling Mode Shapes. *Journal of Marine Science and Application* 18(2):160-166
- [29] Serna MA, Ibáñez JR, López A (2011) Elastic flexural buckling of non-uniform members: Closed-form expression and equivalent load approach. *Journal of Constructional Steel Research* 67(7):1078-85
- [30] Timoshenko S (1955) *Strength of materials*, ed. 3, Princeton NJ: Van Nostrand
- [31] ANSI B (2016) AISC 360-16, Specification for Structural Steel Buildings. Chicago, American Institute of Steel Construction
- [32] ABAQUS Software.